Free Radical Research, October 2009; 43(10): 899–912

informa
healthcare

A class of imidazolium salts is anti-oxidative and anti-fibrotic in hepatic stellate cells

CHUNYAN ZHANG, ZHAOBING DING, NUR-AFIDAH MOHAMED SUHAIMI, YIN LING KNG, YUGEN ZHANG, & LANG ZHUO

Institute of Bioengineering and Nanotechnology, 31 Biopolis Way, The Nanos, Singapore 138669

(Received 2 April 2009; In revised form date 18 June 2009)

Abstract
A class of imidazolium salts (IMSs) is routinely used in organic synthetic chemistry as precursors to generate N-heterocyclic carbenes (NHCs) with catalytic activity. However, their biological properties are largely unknown. The current study investigates the biological activity of a typical NHC precursor DBZIM and its trimer TDBZIM in hepatic stellate cells (HSCs), which is an *in vitro* model for studying liver fibrosis. The results show that HSCs treated with IMSs have an enhanced GSH/GSSG ratio and a reduced level of reactive oxygen species (ROS), which may consequently contribute to the attenuation in gene expression of fibrogenic molecules such as smooth muscle actin-α (SMAA), transforming growth factor-beta 1 (TGF-β1), procollagen αI(I) and fibronectin. Further, the *in vivo* experiments demonstrate that DBZIM is an anti-fibrotic agent in a mouse model of liver fibrosis. These findings suggest that the versatile IMSs could be a potential source for developing novel therapeutics to treat liver fibrosis and other fibrogenic disorders caused by oxidative stress and TGF-β1 mal-signalling.

Keywords: *Imidazolium salts, hepatic stellate cells, hepatic fibrosis, glutathione, TGF-β1, anti-oxidant*

Abbreviations: *IMSs, imidazolium salts; DBZIM, 1,3-bisbenzylimidazolium bromide; TDBZIM, 1,3,5-tris(4-methyl-imidazolium)-linked cyclophane·3Br; GSH, Glutathione; GSSG, disulphide dimer of glutathione; ROS, reactive oxygen species; SMAA, smooth muscle actin-α; HSCs, hepatic stellate cells; TGF-β1, transforming growth factor-beta 1; NHCs, N-heterocyclic carbenes*

Introduction

Hepatic stellate cells (HSCs) are activated by default in response to initial liver injury and may eventually be trans-differentiated to myofibroblast-like cells, if the insult is chronic by nature. This process is characterized by phenotypic changes including cell proliferation, over-expression of smooth muscle actin-α (SMAA) and deposition and abnormal cross-linking of excessive extracellular matrix (ECM) proteins, including collagen type αI (I) (col1a1) and fibronectin. The mechanisms leading to HSC activation and liver fibrogenesis have been studied over the past two decades. Among many cytokines, transforming growth factor-beta 1 (TGF-β1) has been recognized as a major factor responsible for the induction of ECM proteins in the fibrotic liver. HSCs respond to TGF-β1 secreted from Kupffer cells, endothelial cells during liver injury and themselves via autocrine action, resulting in HSC activation and liver fibrogenesis [1].

Oxidative stress resulting from the metabolic generation of reactive oxygen species (ROS) is believed to play an important role in HSC activation and liver fibrogenesis [2,3]. It was shown that products of lipid peroxidation led to an increased synthesis of collagen

Correspondence: Lang Zhuo, PhD, Institute of Bioengineering and Nanotechnology, 31 Biopolis Way, the Nanos, #04-01, Singapore 138669. Tel: (65) 6824-7114. Fax: (65) 6478-9080. Email: lzhuo@ibn.a-star.edu.sg

ISSN 1071-5762 print/ISSN 1029-2470 online
DOI: 10.1080/10715760903137002

by HSCs [4,5]. The potential application of several anti-oxidants as inhibitors of hepatic fibrosis has been examined [6]. (−)-Epigallocatechin gallate (EGCG), a major active component of tea catechin, was shown to suppress HSC activation *in vitro* by inhibiting TGF-β signalling [7–9]. N-acetyl-L-cystein (NAC), a synthetic precursor of glutathione (GSH) used clinically as an antioxidant, displayed anti-fibrogenic property also through suppressing TGF-β signalling [10]. In clinical studies, a combination therapy of vitamins E and C has also been shown to decrease the fibrosis score in non-alcoholic steatohepatitis patients, but did not affect hepatic inflammation [11].

N-heterocyclic carbenes (NHCs) have been widely used as a nucleophilic organo catalyst or universal ligand in synthetic chemistry. Stable NHCs can be generated from imidazolium salts (IMSs) in an aqueous environment. Thus, certain IMSs, such as those used in the current experiment (Table I), are also viewed as NHC precursors. Some attempts to examine the biological applications of this group of materials have been made recently. For example, gold-NHC complex has been reported to induce mitochondrial swelling in a cell-free environment [12]. We recently showed that DBZIM can be converted into NHC and reduce total cellular ROS level [13]. Here we investigate the anti-oxidative mechanisms and assess the anti-fibrotic effect of an additional set of IMSs (Table I) in HSCs.

Materials and methods

Synthesis and characterization of IMSs

The chemical structures of DBZIM (1,3-bisbenzylimidazolium bromide), DBZBIM (1,3-bisbenzylbenzimidazolium bromide) and TDBZIM (1,3,5-tris(4-methyl-imidazolium)-linked cyclophane·3Br) are illustrated in Table I. DBZIM and DBZBIM were synthesized based on a published method [14]. TDBZIM was synthesized by mixing 4-methylimidazole (123 mg, 1.5 mmol) and 2,4,6-tris(bromomethyl)mesitylene (400 mg, 1 mmol) in 200 ml of N,N'-dimethylformamide (DMF) in a reaction vial. The reaction mixture was heated to 100°C for 2 days. Colourless crystals of TDBZIM were precipitated and collected in 40% yield (160 mg). ^{1}H nuclear magnetic resonance (NMR) (400 MHz, CD_3OD): δ 7.77 (s, 1H), 5.53 (s, 2H), 5.41 (s, 2H), 4.60 (s, 1H), 2.55 (s, 3H), 2.19 (s, 6H). ^{13}C NMR (100 MHz, CD_3OD): δ 143.49, 136.27, 131.73, 131.54, 123.45, 67.06, 16.35, 9.57. Elemental analysis for TDBZIM ($C_{36}H_{45}Br_3N_6$): C, 53.21; H, 5.88; N, 10.12 (calc. C, 53.95; H, 5.66; N, 10.49). Additional five IMSs (Table I) were purchased from Sigma Chemicals (St. Louis, MO).

Table I. Chemical structures of IMSs used in the current study.

Name	Abbreviation (IC_{50})	Structure	Name	Abbreviation (IC_{50})	Structure
1,3-Bisbenzylimidazolium bromide	DBZIM (1.7 mM)	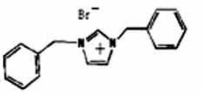	1,3-Bis(1-adamantyl)imidazolium tetrafluoroborate	AMIM (0.17 mM)	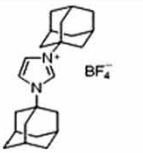
1,3,5-tris(4-methyl-imidazolium)-linked cyclophane·3Br	TDBZIM (0.5 mM)	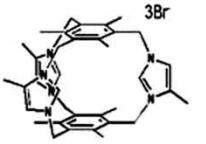	1,3-Bis(2,4,6-trimethylphenyl)-imidazolinium chloride	TMPHIM (0.11 mM)	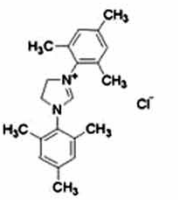
1,3-Diisopropylimidazolium tetrafluoroborate	DPIM (3.1 mM)	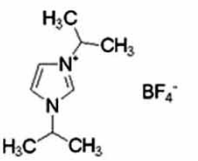	1,3-Bis(2,6-diisopropyl-phenyl)-imidazolinium chloride	DPPHIM (34 μM)	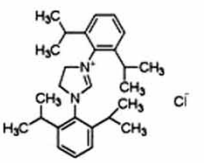
1,3-Di-*tert*-butylimidazolinium tetrafluoroborate	DBIM (2.5 mM)	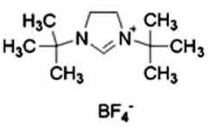	1,3-Bisbenzyl-benzimidazolium bromide	DBZBIM (0.31 mM)	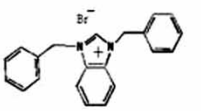

Hepatic stellate cell culture and immunocytochemistry (ICC)

The HSC-T6 cells [15], commonly used as an *in vitro* model for studying hepatic fibrosis, were kindly provided by Dr Scott Friedman of Mount Sinai School of Medicine (New York) and were routinely cultured in DMEM with 10% foetal bovine serum (FBS) in a humidified incubator containing 5% CO_2 at 37°C. The HSCs were grown in DMEM supplemented with 10% FBS on glass cover slips in 24-well culture plates prior to staining with antibodies against SMAA. The cells were washed once with sterile PBS and fixed with 100% methanol for 20 min at 4°C, followed by three washes with PBS. The cells were blocked and permeabilized in blocking solution (10% horse serum, 0.1% Triton X-100 in PBS) for 1 h at 37°C. The cells were incubated with primary antibody SMAA conjugated to Cy3 (Sigma Aldrich, USA) at 1:200 in blocking solution overnight at 4°C. Following overnight incubation, the cells were washed three times with PBS and counterstained with DAPI. Images were acquired with a confocal microscope (LEICA).

Cell proliferation and cytotoxicity assays

The effects of IMSs on HSC-T6 cell proliferation and cytotoxicity were measured using the CellTiter and CytoTox kits (Promega, WI, USA), respectively. The control compounds NAC and EGCG were purchased from Merck KGaA (Germany) and Sigma Chemicals, respectively. Cells were initially seeded in cell culture plates or flasks in DMEM supplemented with 10% FBS for 18–24 h prior to the addition of compounds of various concentrations for different time periods. Final dimethylsulphoxide (DMSO) concentration in the culture medium was kept below 0.2% (v/v). Details of each treatment can be found in the figure legends.

Determination of cellular ROS

The ROS level in HSC-T6 cells was determined using the dichlorofluorescein (DCF) labelling method according to the manufacturer's instructions (Molecular Probes, Inc., OR, USA). The fluorescence readout obtained from a Tecan Safire II plate reader was normalized against viable cell numbers, as determined using a cell viability assay kit (Promega, WI, USA).

Glutathione (GSH) and GSH/disulphide dimer of glutathione (GSSG) assays

Total cellular GSH and GSSG levels were determined by using assay kits from Cayman Chemical (MI, USA) following the manufacturer's instruction. The protein concentration was determined by bicinchonicic acid (BCA) assay. The colourimetric signal was obtained on a Tecan Safire II plate reader. The level of GSH or GSSG was presented as nmol/μg protein.

Glutathione peroxidase (GPx), catalase (CAT) and superoxide dimutase (SOD) assays

For GPx and CAT activities, protein samples were prepared in ice-cold phosphate buffered saline (PBS) containing 1 mM of ethylenediaminetetraacetic acid (EDTA). For SOD activity, protein samples were prepared in 20 mM of N-(2-hydroxyethyl)-piperazine-N′-2-ethanesulfonic acid (HEPES) buffer containing 1 mM of ethylene glycol-bis(2-aminoethylether)-*N*,*N*,*N*′,*N*′-tetraacetic acid (EGTA), 210 mM of mannitol and 70 mM of sucrose. Protein content was determined by BCA assay. The cellular activities of the three anti-oxidant enzymes, GPx, CAT and SOD, were determined using assay kits from Cayman Chemical.

Glutathione S-transferase (GST) assay

The GST activity was assayed using a kit from Cayman Chemical. Total GST (cytosolic and microsomal) activity was measured and presented as nmol/min/mg protein.

Real-time RT-PCR

Total RNA isolation and real-time RT-PCR quantification of mRNAs for SMAA, collagen Ia1, fibronectin, TGF-β1 and TGF-β receptor I (TGFβ RI) were done similarly as previously reported [16] by using the respective Taqman's assays run on the ABI 7500 Fast Real-Time PCR System (Applied Biosystems, CA, USA). Messenger for the rat β-actin gene served as a normalizing reference.

Protein extraction, SDS-PAGE and Western blot

For liver tissue proteins, 30 μg of total protein extracts were further boiled at 95°C for 5 min with 0.1%SDS, resolved in a 4–12% SDS-PAGE gel and transferred onto a nitrocellulose membrane. Primary antibodies SMAA (Sigma Chemicals), Collagen 1a1, Fibronectin (Santa Cruz Biotechnology, CA, USA) and β-actin (Abcam) were used at 1:1000 dilution. Target bands were detected by horseradish peroxidase-conjugated secondary antibody (Santa Cruz Biotechnology). Protein bands were recorded on X-ray film by reacting with ECL chemiluminescence reagents (Amersham Biosciences, NJ, USA). Band intensity was quantified using the SpotDenso density analysis function of the AlphaDigidoc RT software. Similar procedures were used for cellular protein extracts, except that α-tubulin (Abcam, UK) was used as a loading control.

Bile duct ligation (BDL), compound dosing and Sirius Red staining of liver sections

The experimental protocol covering the current study was approved by the Institutional Animal Care and Use Committee. Adult male FVB/N mice (8–10 weeks), which had free access to water and diet, were anaesthetized with Ketamine (150 mg/kg)/Xylazine (10 mg/kg) via i.p. injection. An abdominal incision at the midline was made to expose the common bile conduct, which was then ligated twice using 5-0 silk suture. In the sham-operated animal, the bile duct was exposed, but not ligated. After a two-day recovery from the surgery, mice of different treatment groups were given free access to drinking water containing DBZIM at an indicated concentration (0, 0.8 or 2 g/l) for 4 weeks. The control group had free access to pure drinking water only. At the end of the 4th week, livers from each group ($n = 8$) were removed, after being perfused with 20 ml of PBS buffer, and total proteins extracted for immunoblotting or fixed in 10% formalin prior to paraffin embedding and sectioning.

Paraffin-sections (5 μm in thickness) from the left and median lobes were stained with Sirius Red to visualize the collagen content. After de-waxing, rehydration and air-drying, the sections were stained in 0.1% Sirius Red solution for 1 h, washed twice with 0.5% acetic acid, dehydrated in three changes of ethanol, cleared in xylene and finally mounted with Histomount (National diagnostics, Georgia, USA) for microscopy. The collagen stained areas were digitally captured in six low-magnification ($4\times$) fields from each left and median lobes and were quantified using the Image J software according to the instructions.

Statistical analysis

All quantitative results were presented as mean $\pm$ SEM (standard error of the mean). Experimental data were analysed using two-tailed Student's *t*-test assuming unequal variances. A *p*-value of ≤ 0.05 was considered statistically significant.

Results

DBZIM and TDBZIM had low cytotoxicity

We first assessed the effects of DBZIM and TDBZIM on the proliferation of HSC-T6 cells treated with the two compounds separately for 48 h. DBZIM at 250–400 μM and TDBZIM at 125–200 μM moderately inhibited cell proliferation by 3.5–8.9% and 13–19%, respectively (Figure 1A and B). Higher concentrations of DBZIM (400–1000 μM) began to show some

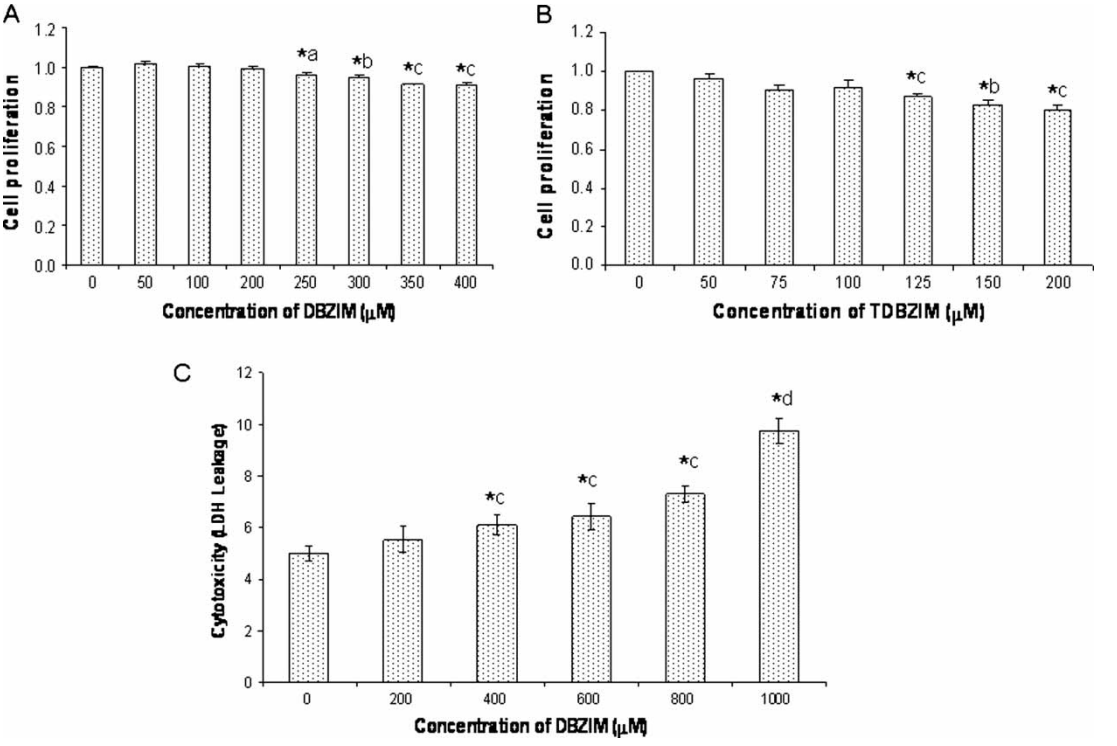

Figure 1. Proliferation and cytotoxicity assays on DBZIM and TDBZIM. (A) The HSC-T6 cells were initially seeded at a density of 5000 cells/well in 96-well plates in DMEM medium supplemented with 10% FBS for 18–24 h. Subsequently DBZIM was added to the culture at final concentrations of 0–400 μM and the cells were further cultured for an additional 48 h prior to the proliferation assay (Promega's CellTiter kit). (B) TDBZIM was similarly assayed in the range of 0–200 μM. A moderate (but statistically significant) inhibition of cell proliferation was noted for the two compounds at high concentrations. (C) The cytotoxicity of DBZIM (0–1000 μM) was assayed at 48 h using the CytoTox kit (Promega). A significant toxicity was observed for cells treated with this compound at high concentrations. The data presented here were from four independent experiments; they were presented as mean and SEM, *a $p < 0.05$, *b $p < 0.01$, *c $p < 0.005$ and *d $p < 0.0005$.

sign of cytotoxocity, as assayed for LDH leakage (Figure 1C).

DBZIM and TDBZIM simultaneously attenuated cellular ROS and enhanced GSH/GSSG ratio

To measure the influence of IMSs on the cellular oxidative stress level, the HSC-T6 cells treated with DBZIM (10, 50, 100 and 300 μM) or TDBZIM (10, 50 and 100 μM) for 48 h in full serum medium were assayed for ROS, GSH and GSSG, using NAC (1 or 5 mM) and EGCG (25 μM) as references. As shown in Figure 2, the cellular ROS level was significantly reduced by 25% by 300 μM of DBZIM ($p < 0.005$; Figure 2A) or by 34% by 100 μM of TDBZIM ($p < 0.0005$; Figure 2B) in a dosage-dependent manner. For comparison, EGCG attenuated the ROS level by a moderate 14% at 25 μM ($p < 0.005$), while NAC (1 mM) did not show an apparent inhibition on the ROS level.

We also investigated the perturbation effect of the exogenous DBZIM and TDBZIM on the level of a key endogenous anti-oxidant, GSH. Figure 3A and B quantified the total amount of cellular GSH including the reduced glutathione (GSH) and the oxidized glutathione (GSSG). As shown in Figure 3A, DBZIM actually reduced the total GSH level by 12% ($p < 0.005$) and 20% ($p < 0.0001$) at 50 and 100 μM, respectively. However a higher concentration of DBZIM (300 μM) did not significantly change the GSH level. For comparison, NAC (5 mM) did not show any effect on the total GSH, while EGCG (25 μM) increased the GSH level by 19% ($p < 0.01$), which was thought to occur via a *de novo* synthesis [8]. On the other hand, TDBZIM (10–100 μM) did not alter the total cellular GSH level (Figure 3B). At the same time, the DBZIM (10–300 μM) and TDBZIM (10–100 μM) treatments led to had significantly lower levels of GSSG (Figure 3C and D) and a higher GSH/GSSG ratio (Figure 3E and F). In particular, 300 μM of DBZIM dramatically increased the GSH/GSSG ratio to 7.4-fold of the control.

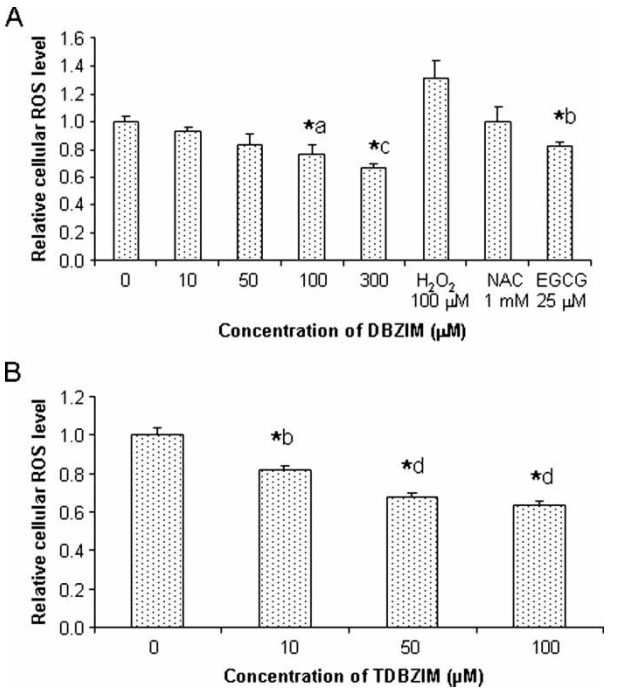

Figure 2. DBZIM and TDBZIM attenuated total cellular ROS level. (A) The HSC-T6 cells were incubated with DBZIM (10, 50, 100 and 300 μM), with 100 μM of H_2O_2, NAC (1 mM) and EGCG (25 μM) as controls for 48 h prior to ROS assay. (B) TDBZIM at slightly lower concentrations (10, 50 and 100 μM) was subject to the similar treatment and assay as in (A). All data were presented as relative values in mean ($n = 6$) and SEM. *a $p < 0.05$, *b $p < 0.01$, *c $p < 0.005$ and *d $p < 0.0005$, when compared to the vehicle control value normalized to 1.

DBZIM and TDBZIM attenuated GPx and CAT, but induced GST activity

We further measured the activity of several key anti-oxidant enzymes, GPx, CAT and SOD, under the influence of either DBZIM or TDBZIM. As shown in Figure 4A, DBZIM slightly attenuated the GPx activity by 10% at 10–50 μM, but enhanced the GPx activity at 300 μM by 15% ($p < 0.005$), displaying a mild biphasic pattern. TDBZIM (10–100 μM) dose-dependently suppressed the GPx activity (Figure 4B). As controls, EGCG (25 μM) was found to reduce the GPx activity by 53% ($p < 0.005$), while NAC (5 mM) did not have a significant influence on the GPx activity (Figure 4B). Similarly DBZIM and TDBZIM had a moderate attenuating effect on the CAT activity (Figure 4C and D). As controls, EGCG (25 μM) had no impact on the CAT activity, while NAC (5 mM) surely inhibited the CAT activity by 35% ($p < 0.01$). Under the assay conditions used, DBZIM or TDBZIM had no effect on the SOD activity (Figure 4E and F). Finally in this category, the GST activity (Figure 4G) was found to be induced by DBZIM (100–300 μM).

DBZIM and TDBZIM suppressed HSC activation marker and fibrogenic molecules

We next investigated the ability of DBZIM and TDBZIM to inhibit HSC activation. Real-time RT-PCR data showed that DBZIM and TDBZIM suppressed the transcription of SMAA, procollagen αI(I) and fibronectin in a dosage-dependent (Figure 5A and B) and a time-dependent (Figure 6A–C) manner. At the protein level, DBZIM (100 μM) also suppressed SMAA and fibronectin significantly at 48 h (Figure 6D).

DBZIM and TDBZIM suppressed TGF-β1 and TGF β RI expression

To see whether the DBZIM and TDBZIM conferred their anti-fibrotic effect by inhibiting TGF-β1

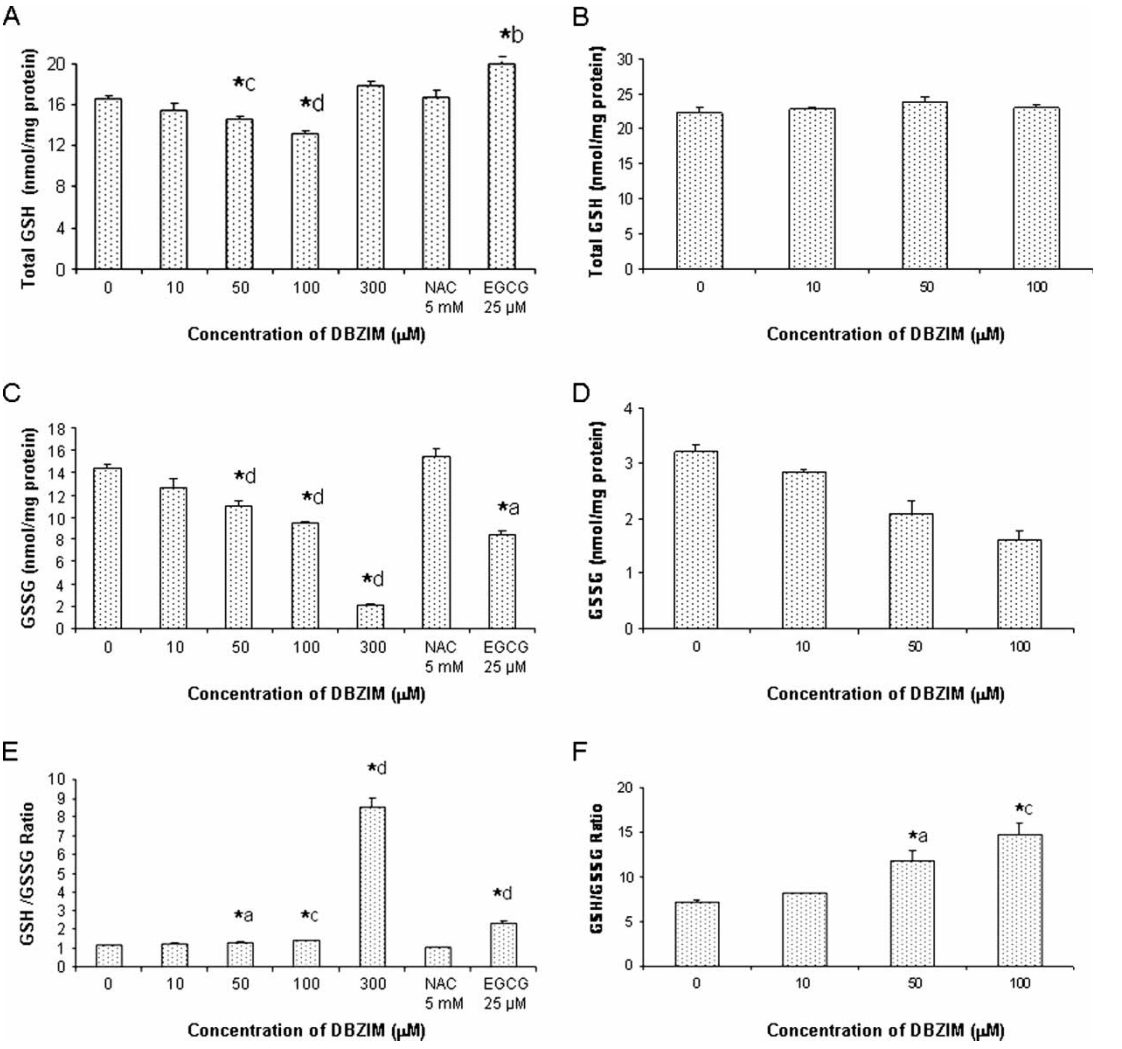

Figure 3. Effects of DBZIM and TDBZIM on total cellular GSH level and the GSH/GSSG ratio. The HSC-T6 cells were incubated with various concentrations of DBZIM or TDBZIM for 48 h and assayed for the total GSH and GSSG. (A) DBZIM slightly attenuated the total cellular GSH level in the 50–100 μM range; (B) TDBZIM did not change the total GSH level; (C) DBZIM and (D) TDBZIM both at the μM range suppressed the level of cellular GSSG (the oxidation product of GSH); by calculation, both DBZIM (E) and TDBZIM (F) enhanced the GSH/GSSG ratio. The GSH and GSSG amounts were normalized against the total protein. The data were presented as mean and SEM, $n = 6$, *a $p < 0.05$, *b $p < 0.01$, *c $p < 0.005$ and *d $p < 0.0005$, when compared to the vehicle control.

signalling, we measured the TGF-β1 mRNA levels in cells treated with DBZIM (100–300 μM) and TDBZIM (1–100 μM) and found that both IMSs significantly reduced the TGF-β1 transcript in a dose-dependent (Figure 7A and B) and a time-dependent fashion (Figure 7C).

DBZIM attenuated H_2O_2-induced activation and proliferation of HSC-T6 cells

We recently showed that IMSs can scavenge ROS in a cell-free environment [13]. Here we specifically investigated the ability of DBZIM to attenuate the oxidative stress of hydrogen peroxide in cultured HSCs. As expected, HSC-T6 cells treated with 100 μM of H_2O_2 were at a more activated state (Figure 8A), as shown by ICC using with a SMAA antibody, when compared to the vehicle (0.1% DMSO) control. More critically, cells co-treated with H_2O_2 and DBZIM displayed a less intense staining for SMAA. In addition, DBZIM also significantly reduced the H_2O_2-induced proliferation in a dose-dependent manner (Figure 8B).

DBZIM decreased activation marker and ECM proteins in the liver of BDL-mice

To investigate whether the anti-fibrotic property of IMSs, as observed *in vitro*, is preserved *in vivo*, DBZIM was administered to BDL-mice through drinking water for 4 weeks. Quantification of collagen content (by Sirius Red stain) from the liver sections showed that DBZIM (2 g/l) significantly reduced the total collagen content in the BDL-mice

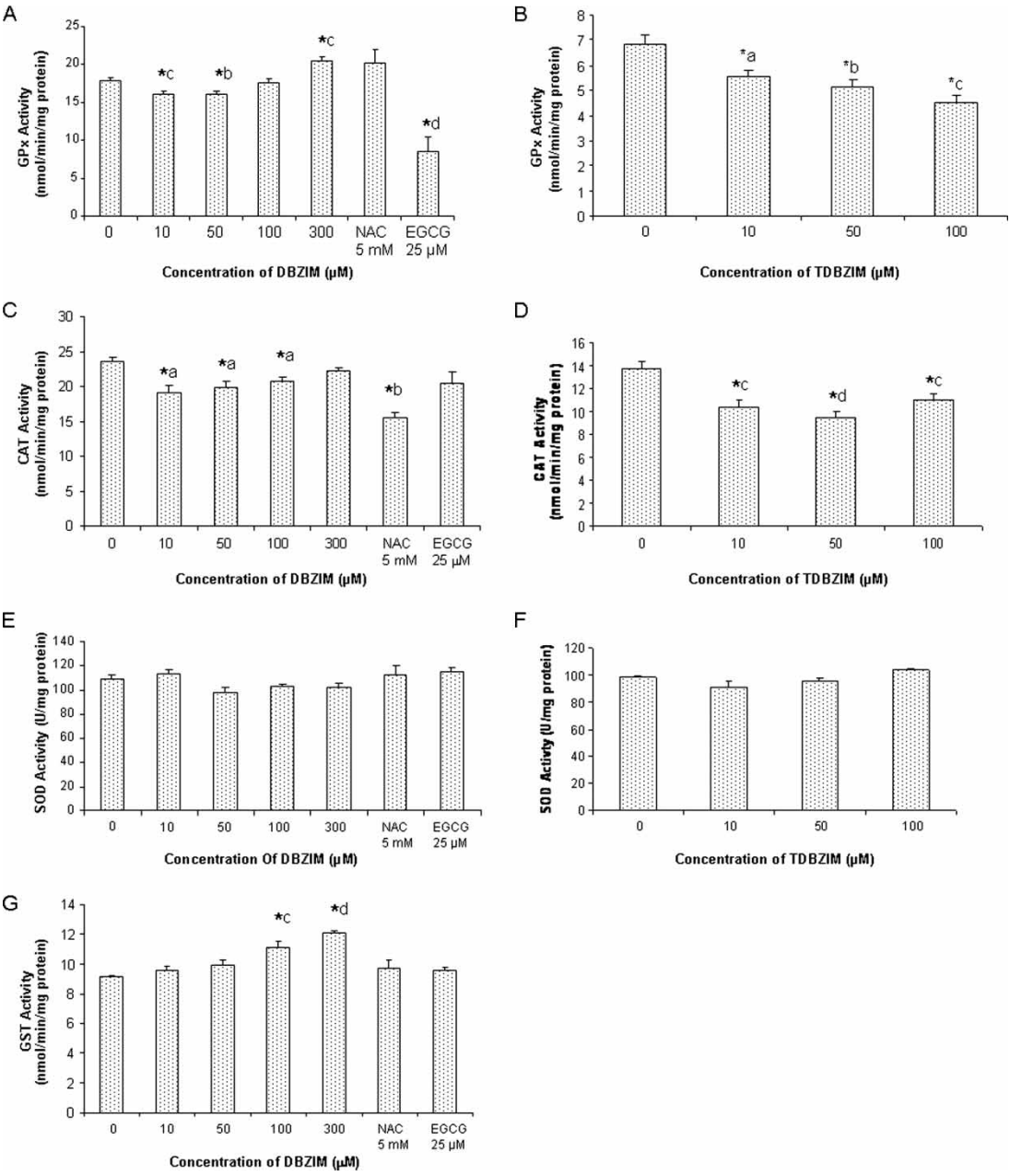

Figure 4. Effects of DBZIM and TDBZIM on the total cellular activity of four anti-oxidant enzymes. The HSC-T6 cells were treated with compounds of various concentrations for 48 h and homogenized by sonication (60% frequency for 30 s) in PBS (pH 7.4, 1 mM of EDTA) for GPx, GST and CAT assays or in 20 mM of HEPES buffer containing 1 mM of EGTA, 210 mM of mannitol and 70 mM of sucrose (pH 7.2) for SOD assay. The GPx activity was reduced slightly by DBZIM (A) and moderately by TDBZIM (B). The CAT activity was reduced similarly by DBZIM (C) and TDBZIM (D). The SOD activity however was not affected by either DBZIM (E) or TDBZIM (F). (G) The GST activity was induced by DBZIM (100–300 μM). The data were presented as mean and SEM, $n = 6$, *a $p < 0.05$, *b $p < 0.01$, *c $p < 0.005$ and *d $p < 0.0005$, when compared to the vehicle control.

by 60% at the end of the 4-week treatment ($p < 0.05$) and, at the same time, the DBZIM (2 g/l) treatment alone did not change the collagen content in the sham mice (Figure 9A and B). DBZIM at a lower concentration (0.8 g/l) also showed some inhibitory effect, but did not achieve a significant level. At the molecular level, immunoblotting of liver proteins revealed that DMZIM (2 g/l) significantly decreased the protein level of collagen 1a1, fibronectin and SMAA by 63% ($p < 0.0001$), 73% ($p < 0.001$) and 64% ($p < 0.01$; Figure 9C and D), respectively.

Cytotoxicity and anti-fibrotic property of additional IMSs

In addition to DBZIM and TDBZIM, six other IMSs with different substituents (Table I) were also tested in HSC-T6 cells to assess cytotoxicity. In general, those with smaller aliphatic groups, such as 1,3-diisopropylimidazolinium tetrafluoroborate (DPIM) and 1,3-di-*tert*-butylimidazolium tetrafluoroborate (DBIM), showed less cytotoxicity, compared to those with bulky aromatic groups, such as 1,3-bis(2,4,6-trimethylphenyl)imidazolium chloride (TMPHIM)

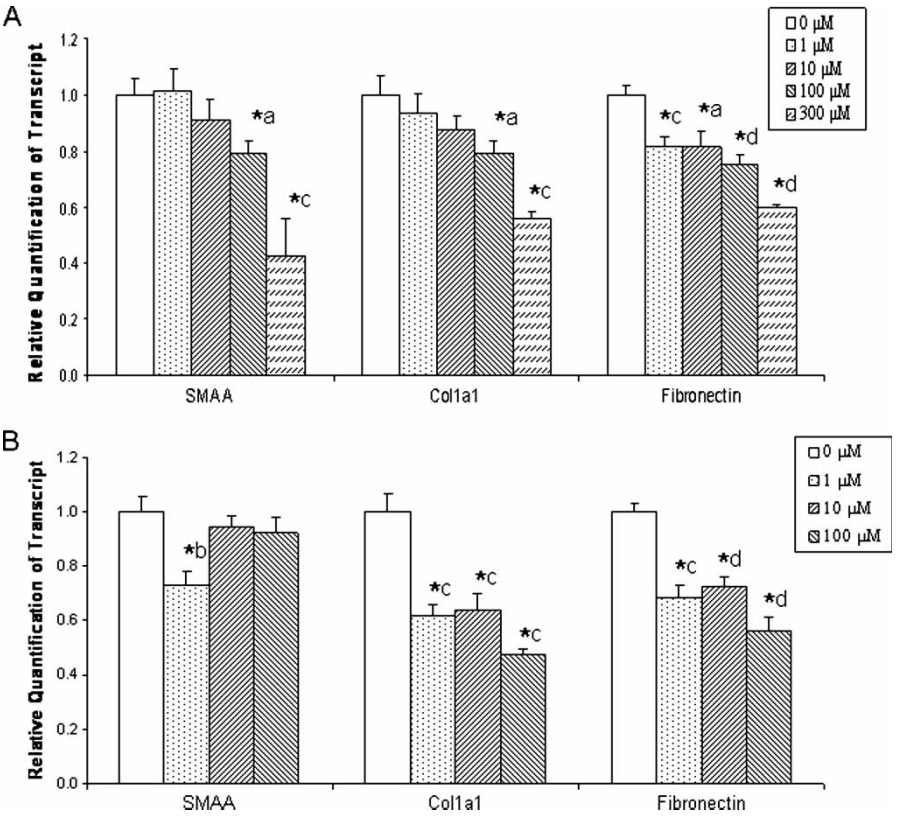

Figure 5. DBZIM (A) and TDBZIM (B) suppressed gene transcription of HSC activation marker SMAA and fibrotic end points (Col1a1 and fibronectin) in a dosage-dependent manner. The HSC-T6 cells were treated with DBZIM (1, 10, 100 and 300 μM) and TDBZIM (1, 10 and 100 μM) for 48 h. Messengers for individual genes were quantified by real-time RT-PCR method using β-actin as a reference. The data were presented as mean and SEM, $n=6$, *a $p<0.05$, *b $p<0.01$, *c $p<0.005$ and *d $p<0.0005$, when compared to the vehicle control.

and 1,3-bis(2,6-diisopropylphenyl)imidazolium chloride (DPPHIM). Those with a methyl spacer between the imidazolium and aromatic ring, such as DBZIM and 1,3-bisbenzylbenzimidazolium bromide (DBZBIM), had moderate cytotoxicity. For comparison, the cytotoxicity (IC_{50} value) of all eight IMs was listed in Table I.

The anti-fibrotic property of the additional IMSs was evaluated in the HSC-T6 cells using a concentration below their respective IC_{50}. Individual IMs were either dissolved in DMSO or H_2O depending on their solubility. At the transcript level, several IMSs, particularly DPIM, significantly reduced the mRNA level for SMAA, Col1a1 and fibronectin at 48 h (Figure 10). At the protein level, all IMSs demonstrated a certain degree of anti-fibrotic efficacy by reducing the protein level of five important fibrogenic molecules (SMAA, Col1a1, fibronectin, TGF-β1 and TGFβ RI) (Figure 11). The densitometric measurements of the protein blots (Figure 11) were summarized in Table II. In an over-simplified model, in which all five parameters (molecules) weigh equally, the *in vitro* efficacy of individual IMSs (at the concentrations used) and EGCG could be roughly ranked as DPIM > TMPHIM > EGCG > AMIM > DBZBIM > DBZIM > DPPHIM.

Discussion

IMSs have low cytotoxicity

One of the primary concerns in developing synthetic anti-oxidants for therapeutic application is the potential cytotoxicity. The IC_{50} values (Table I) for most of the IMSs compared favourably to those (25–75 μM) for two common anti-oxidants, EGCG and genistein [7,16]. The moderate cytotoxicity of the IMSs would certainly provide some confidence in synthesizing additional IMS candidates with novel properties and functionalities tailored to specific therapeutic needs.

IMSs' anti-oxidative property is mediated through the neutralization of ROS

Anti-oxidants exert their effects mainly through three different pathways: (1) neutralization of cellular ROS generated during metabolism and immune response; (2) induction of endogenous anti-oxidative enzymatic activity; and (3) chelation of iron or copper ions that catalyse the generation of hydroxyl radical. GPx, CAT and SOD, which constitute the first line of cellular anti-oxidative defense, are directly involved in the neutralization of ROS. GPx enzyme reduces H_2O_2 to H_2O, while GSH functions as a cofactor

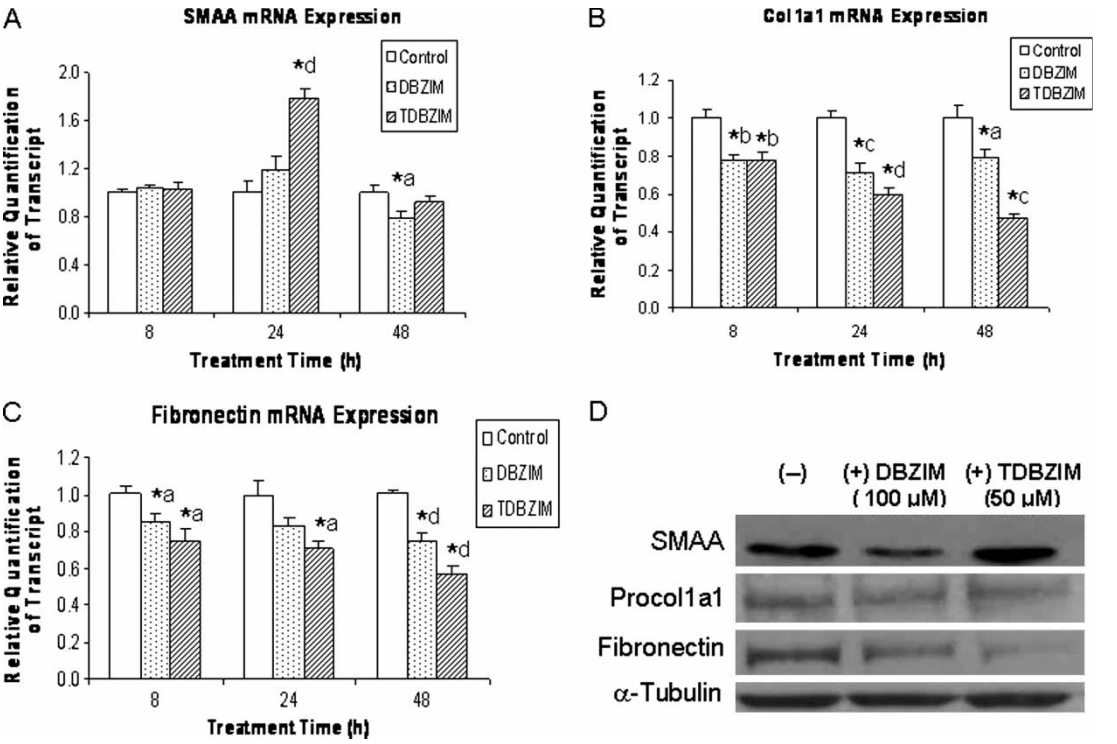

Figure 6. DBZIM (100 μM) and TDBZIM (100 μM) reduced mRNA level for (A) SMAA, (B) Col1a1 and (C) fibronectin in a time-dependent manner. The HSC-T6 cells were treated with DBZIM or TDBZIM and harvested after 8, 24 and 48 h for mRNA quantification by real-time RT-PCR method using β-actin as a reference. (D) DBZIM (100 μM) and TDBZIM (50 μM) also reduced fibrotic marker and end point proteins SMAA, Col1a1 and fibronectin protein expression for 48 h. α-tubulin was used as a reference. The data were presented as mean and SEM, $n=6$, *a $p<0.05$, *b $p<0.01$, *c $p<0.005$ and *d $p<0.0005$, when compared to the vehicle control.

and is consequently oxidized to GSSG. CAT is a peroxisomal enzyme and converts H_2O_2 to H_2O. Our experimental data showed that DBZIM can significantly neutralize the oxidative stress imposed by exogenous H_2O_2 on the HSCs, as a less intense SMAA staining and a lower proliferation were in cells co-treated with H_2O_2 and DBZIM, compared to cells treated with H_2O_2 alone (Figure 8A). SOD

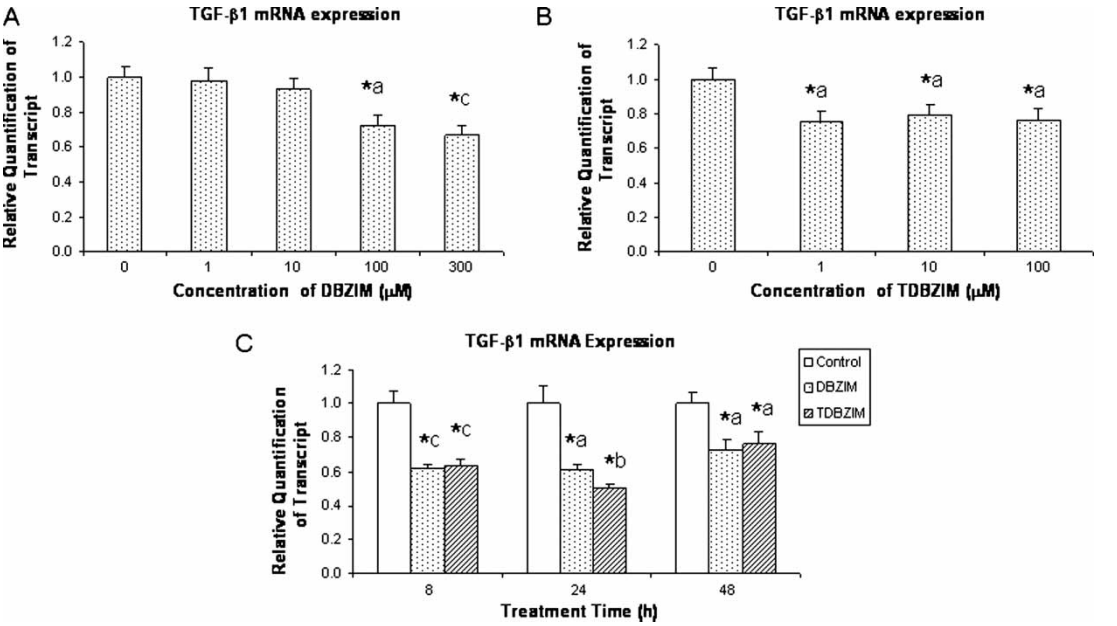

Figure 7. DBZIM and TDBZIM suppressed TGF-β1 mRNA. The HSC-T6 cells treated with (A) DBZIM (1, 10, 100 and 300 μM) or (B) TDBZIM (1, 10 and 100 μM) for 48 h were harvested for the dosage-dependent study at the transcriptional level by real-time RT-PCR method. Both DBZIM (100–300 μM) and TDBZIM (1–100 μM) significantly suppressed TGF-β1 expression when assayed at 48 h. In (C), DBZIM (100 μM) and TDBZIM (100 μM) time-dependently suppressed the TGF-β1 mRNA, when assayed at 8, 24 and 48 h. The data were presented as mean and SEM, $n=6$, *a $p<0.05$, *b $p<0.01$, *c $p<0.005$, when compared to vehicle control.

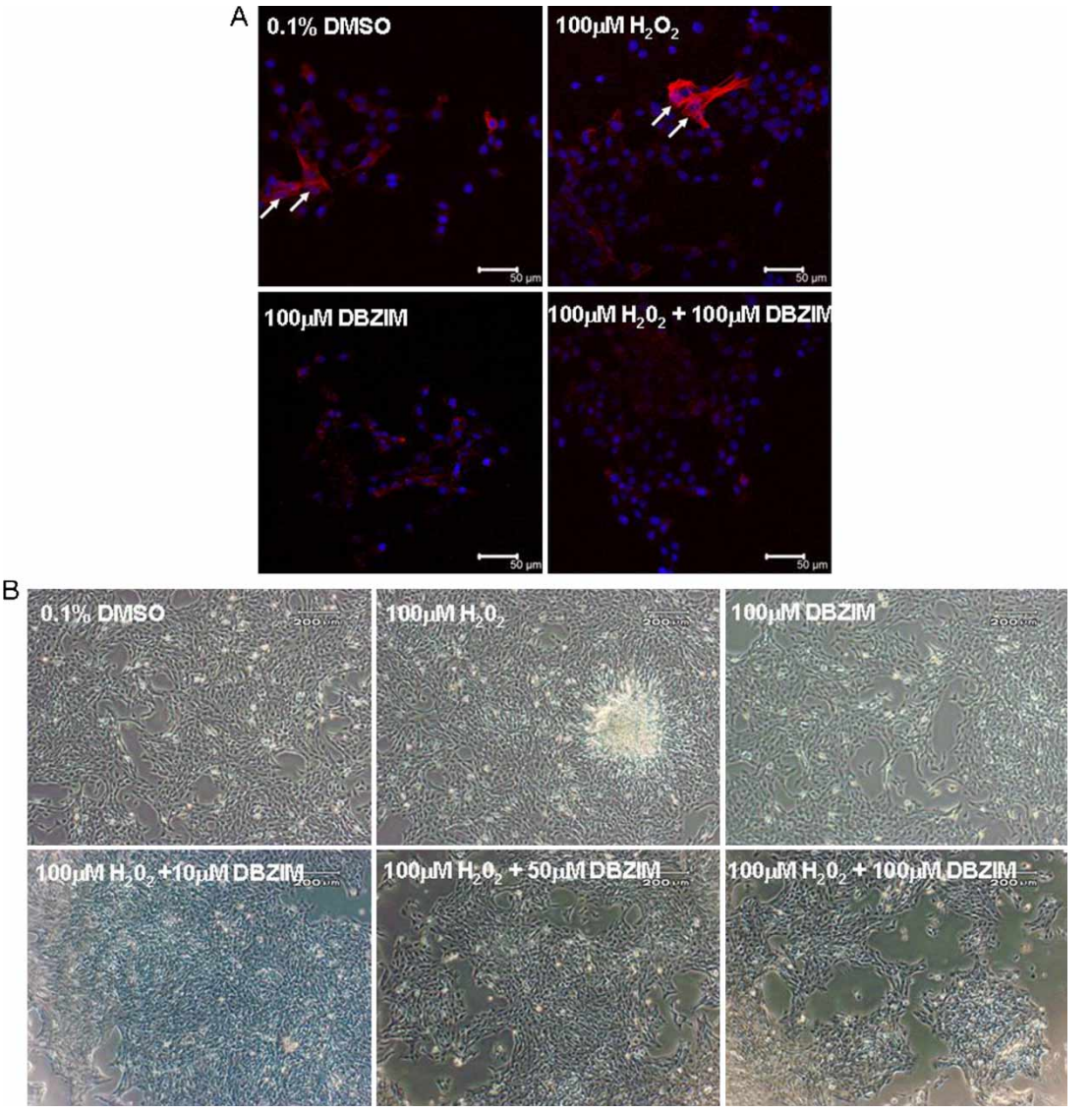

Figure 8. DBZIM inhibited the H_2O_2-induced activation and proliferation of cultured HSCs. (A) ICC showed that while most of the HSC-T6 cells in the 0.1% DMSO vehicle control were at a basal activation state, some of the cells (arrows) were at a higher activation state. Addition of 100 μM H_2O_2 triggered some of the cells (arrows) to an even higher activation state, as shown by the intense SMAA staining. More importantly, DBZIM (100 μM) effectively inhibited the H_2O_2-induced HSC activation. It was also evident that DBZIM dose-dependently inhibited the H_2O_2-induced HSC profileration (B).

catalyses the dismutation of superoxide. We showed that IMSs effectively attenuated ROSs (in particular H_2O_2 and lipid peroxides), which reacted to 2′,7′-dichloro-fluorescein diacetate (DCF-DA) probe [17] in a dosage-dependent manner (Figure 2). While the total GSH level remained relatively constant, the amount of GSSG was dramatically reduced by IMSs, resulting in a significant increase in the GSH/GSSG ratio. We showed in a separate study [13] that IMSs could be converted to NHCs in an aqueous environment and acted as free radical scavengers. It was demonstrated in the cell-free environment that the strong capacity of a particular IMS to reduce gold solution to gold nanoparticles is related to its robust electron-donating ability and with less a sterically hindered substituent, such as DBZIM. It was shown in the current study that the reducing and free radical scavenging power of IMSs are not only preserved in cells, but also influence fibrogenic signalling pathways in HSCs *in vitro* and *in vivo*. However it is entirely speculative whether some IMSs (e.g. DBZIM) could function as catalytic antioxidants in cells and tissues, despite the fact that IMSs can be converted to NHCs and act as catalysts in organic chemistry synthesis. Interestingly we also observed a slight attenuation in the GPx and CAT activity by IMSs (Figure 4). We reason that since a significant amount of ROSs was already neutralized by the addition of IMSs, the burden on cellular antioxidative defense, which was borne by GPx and CAT, was lessened to a point even lower than that of the control. In the literature, a reduction in GPx, CAT and SOD was also reported in the reversion of an experimental cholestasis by administering

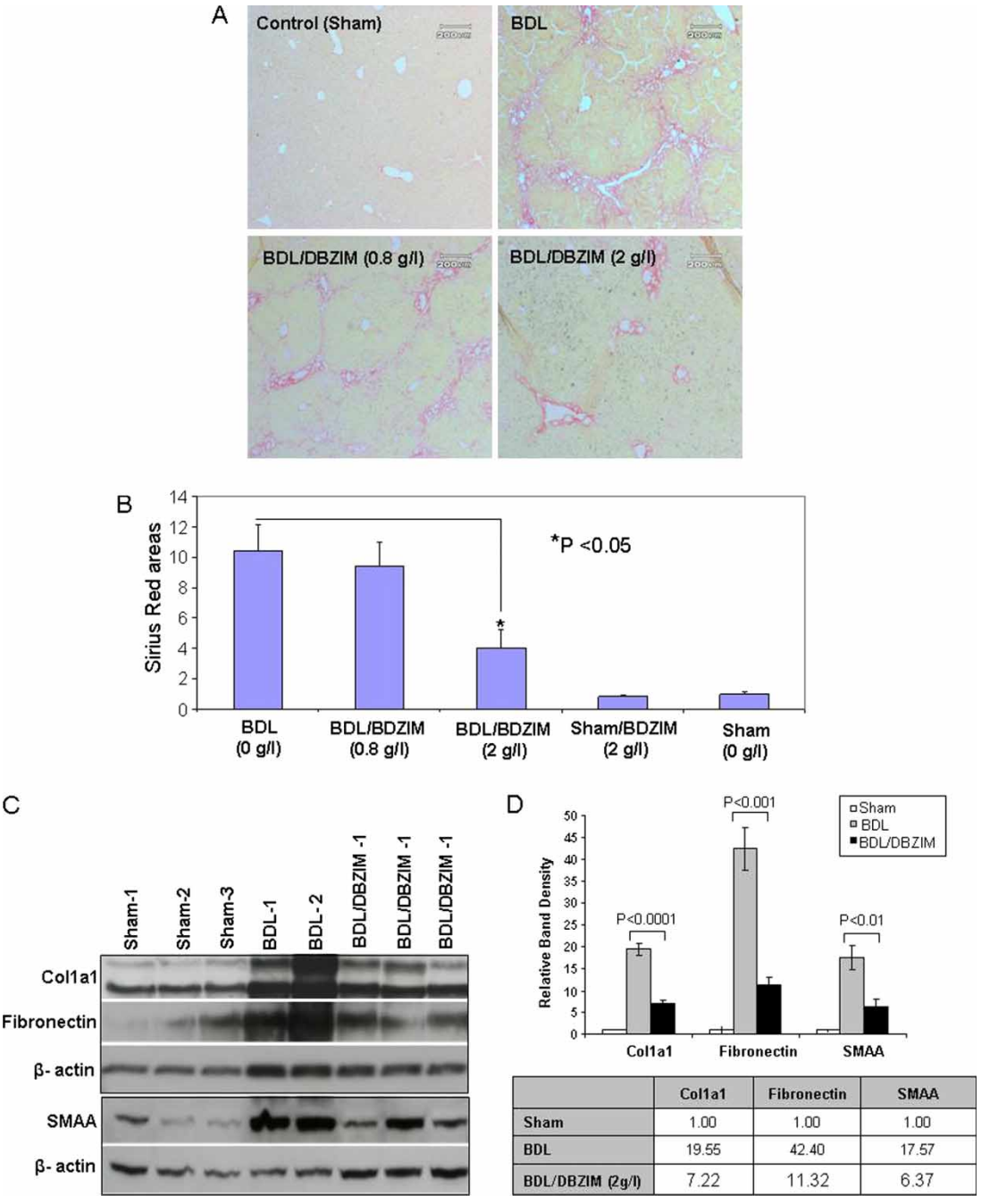

	Col1a1	Fibronectin	SMAA
Sham	1.00	1.00	1.00
BDL	19.55	42.40	17.57
BDL/DBZIM (2g/l)	7.22	11.32	6.37

Figure 9. DBZIM significantly attenuated the BDL-induced collagen accumulation in the sinusoidal areas (A) and quantification (B) of Sirius Red stained areas confirmed this observation; Immunoblotting of liver proteins with antibodies against Col 1a1, fibronectin and SMAA (C) and quantification of protein bands (D) confirmed the suppression of key fibrogenic molecules by DBZIM treatment *in vivo*.

anti-oxidative melatonin [18]. On the other hand, the slight induction in the GST activity (Figure 4G) by DBZIM (100–300 μM) may suggest that DBZIM could help to restore and replenish the detoxifying GST activity that was diminished in the culturally activated HSCs [19].

IMSs are anti-fibrotic

EGCG was shown to suppress TGF-β1 signalling in HSCs by decreasing the active form of TGF-β1 [8], while NAC was shown to inhibit TGF-β1 signalling at distinct molecular steps, including blocking TGF-β1 binding to endoglin, a component in TGF-β1 receptor complex [10]. Although all eight IMSs showed anti-fibrotic property of a varying degree (Figure 11 and Table II), the mechanism(s) on how individual IMS or IMSs as a class influence TGF-β1 signalling and ECM production remain unclear at the moment. Further studies, especially in animal models of hepatic fibrosis, are needed in order to gain mechanistic insights into this class of compounds.

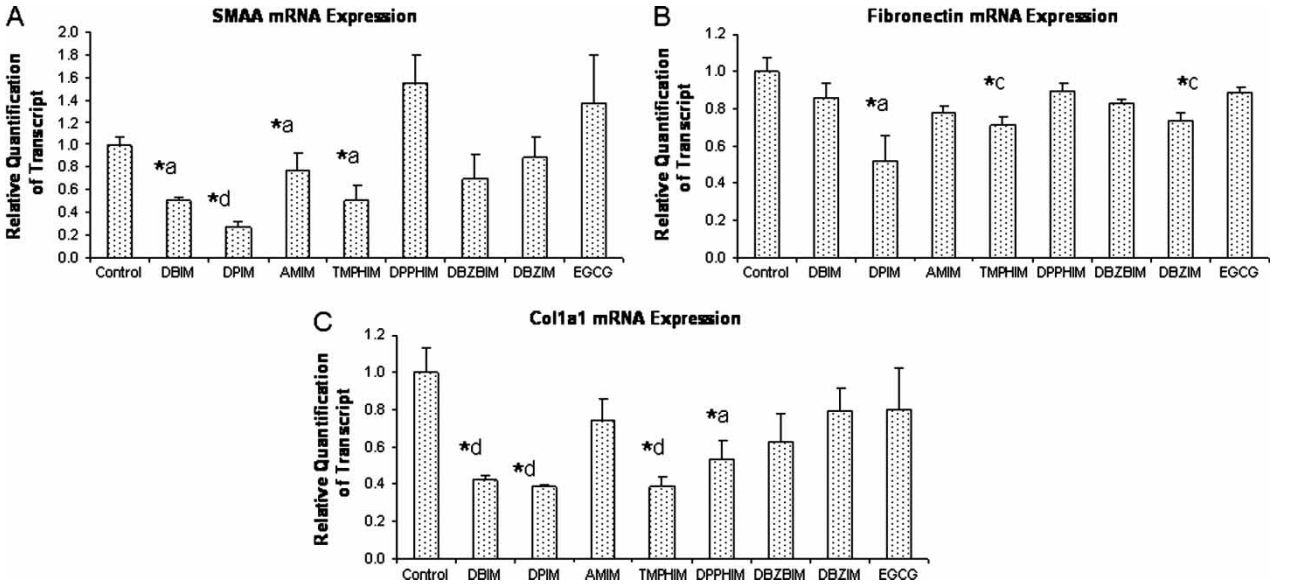

Figure 10. Transcriptional assay of additional members of IMSs. The HSC-T6 cells were treated with various concentrations of IMSs for 48 h and subsequently quantified for mRNA level using real-time RT-PCR method for (A) SMAA, (B) fibronectin and (C) col1a1. DBIM (1 mM), AMIM (50 μM), TMPHIM (50 μM), DPPHIM (10 μM) and DBZBIM (100 μM) were dissolved in DMSO with a final DMSO concentration of 0.2% (v/v). DPIM (2 mM), EGCG (25 μM) and DBZIM (100 μM) were dissolved in water. The data were presented as mean and SEM, $n=6$, *a $p<0.05$, *c $p<0.005$ and *d $p<0.0005$, when compared to the vehicle control.

IMSs as drug-like compounds

ROS has been implicated in a number of pathophysiological conditions, including liver fibrosis, neurological disorders, cardiovascular diseases, cancers and ageing, etc. Therefore, anti-oxidation has been pursued as a therapeutic strategy for a number of diseases. For example, a number of natural anti-oxidants including resveratrol [20] and EGCG [21] have been tested for health benefits and disease-fighting capability. However, a stringent scientific proof for using natural anti-oxidants as therapeutics has not been established [22] due to a number of factors, including low potency and rapid turnover in the body. For example, it was reported that the half-life of EGCG was only ~30 min in the culture medium for human oesophageal cancer cells [23] and ~72 min in rat blood [24]. Alternatively, natural anti-oxidants have been chemically modified to enhance their potency [25]. Synthetic mimics of SOD and catalase have also been developed and shown to be effective in rodent models of ischemia and Parkinson's disease [26]. By comparison, less effort has been devoted to fully synthetic anti-oxidants. One of a few exceptions was that a class of nitron-free radical trap agents, alpha-phenyl-N-tert-butyl-nitron (PBN) and disodium 2,4-disulphophenyl-N-tert-butylnitrone (NXY-059) have been extensively studied and shown to be a potent neuroprotective agent [27] and an anti-cancer agent [28].

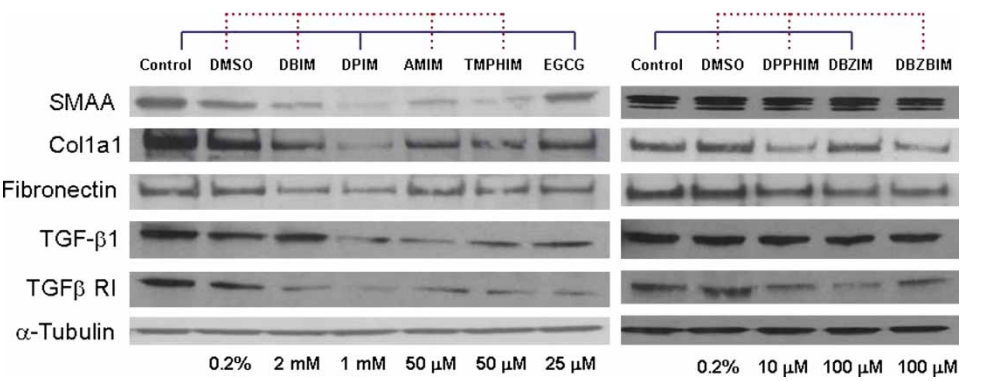

Figure 11. Protein assay of additional members of IMSs. The HSC-T6 cells were treated with various concentrations of IMSs for 48 h and subsequently quantified for protein level using Western blot method for SMAA, Col1a1, fibronectin, TGF-β1 and TGFβ RI, using α-tubulin as a reference. DBIM (1 mM), AMIM (50 μM), TMPHIM (50 μM), DPPHIM (10 μM) and DBZBIM (100 μM) were dissolved in DMSO (dotted line) with a final DMSO concentration of 0.2% (v/v). DPIM (2 mM), EGCG (25 μM) and DBZIM (100 μM) were dissolved in water (solid line). The data were presented as mean and SEM, $n=6$, *a $p<0.05$, *c $p<0.005$ and *d $p<0.0005$, when compared to the vehicle control.

Table II. Relative densitometric measurement of protein bands in Figure 11. The band intensity for the respective control was normalized to 1.

	DBIM (2mM)	DPIM (1 mM)	AMIM (50 μM)	TMPHIM (50 μM)	DPPHIH (10μM)	DBZIM (100 μM)	DBZBIM (100 μM)	EGCG (25 μM)
SMAA	0.50	0.18	0.42	0.34	0.85	0.94	0.75	0.77
Col1a1	0.64	0.28	0.64	0.61	0.55	0.87	0.52	0.61
Fibronectin	0.58	0.53	0.96	0.70	0.82	0.67	0.71	0.55
TGF-β1	1.03	0.33	0.29	0.49	0.94	0.81	1.01	0.53
TGF-β R1	0.35	0.19	0.45	0.35	0.65	0.37	0.45	0.23

Adding to the short but growing list of synthetic antioxidants are the IMSs as described in the current report. Particularly DBZIM has been shown be an effective anti-fibrotic agent *in vitro* and in a mouse model of liver fibrosis. These preliminary observations should warrant future efforts in investigating this class of compounds in animal models of hepatic fibrosis.

Acknowledgements

This research was supported by the Institute of Bioengineering and Nanotechnology (IBN) (Biomedical Research Council, Agency for Science, Technology and Research, Singapore). The authors thank Ms. Siti Nurhanna Riduan for technical assistance in chemical synthesis.

Declaration of interest: The authors report no conflicts of interest. The authors alone are responsible for the content and writing of the paper.

References

[1] Bachem MG, Meyer D, Melchior R, Sell KM, Gressner AM. Activation of rat liver perisinusoidal lipocytes by transforming growth factors derived from myofibroblastlike cells. A potential mechanism of self perpetuation in liver fibrogenesis. J Clin Invest 1992;89:19–27.

[2] Britton RS, Bacon BR. Role of free radicals in liver diseases and hepatic fibrosis. Hepatogastroenterology 1994;41: 343–348.

[3] Galli A, Svegliati-Baroni G, Ceni E, Milani S, Ridolfi F, Salzano R, Tarocchi M, Grappone C, Pellegrini G, Benedetti A, Surrenti C, Casini A. Oxidative stress stimulates proliferation and invasiveness of hepatic stellate cells via a MMP2-mediated mechanism. Hepatology 2005;41:1074–1084.

[4] Casini A, Ceni E, Salzano R, Biondi P, Parola M, Galli A, Foschi M, Caligiuri A, Pinzani M, Surrenti C. Neutrophil-derived superoxide anion induces lipid peroxidation and stimulates collagen synthesis in human hepatic stellate cells: role of nitric oxide. Hepatology 1997;25:361–367.

[5] Parola M, Pinzani M, Casini A, Leonarduzzi G, Marra F, Caligiuri A, Ceni E, Biondi P, Poli G, Dianzani MU. Induction of procollagen type I gene expression and synthesis in human hepatic stellate cells by 4-hydroxy-2,3-nonenal and other 4-hydroxy-2,3-alkenals is related to their molecular structure. Biochem Biophys Res Commun 1996;222: 261–264.

[6] Kawada N, Seki S, Inoue M, Kuroki T. Effect of antioxidants, resveratrol, quercetin, and N-acetylcysteine, on the functions of cultured rat hepatic stellate cells and Kupffer cells. Hepatology 1998;27:1265–1274.

[7] Chen A, Zhang L, Xu J, Tang J. The antioxidant (−)-epigallocatechin-3-gallate inhibits activated hepatic stellate cell growth and suppresses acetaldehyde-induced gene expression. Biochem J 2002;368:695–704.

[8] Yumei F, Zhou Y, Zheng S, Chen A. The antifibrogenic effect of (−)-epigallocatechin gallate results from the induction of *de novo* synthesis of glutathione in passaged rat hepatic stellate cells. Lab Invest 2006;86:697–709.

[9] Nakamuta M, Higashi N, Kohjima M, Fukushima M, Ohta S, Kotoh K, Kobayashi N, Enjoji M. Epigallocatechin-3-gallate, a polyphenol component of green tea, suppresses both collagen production and collagenase activity in hepatic stellate cells. Int J Mol Med 2005;16:677–681.

[10] Meurer SK, Lahme B, Tihaa L, Weiskirchen R, Gressner AM. N-acetyl-L-cysteine suppresses TGF-beta signaling at distinct molecular steps: the biochemical and biological efficacy of a multifunctional, antifibrotic drug. Biochem Pharmacol 2005;70:1026–1034.

[11] Harrison SA, Torgerson S, Hayashi P, Ward J, Schenker S. Vitamin E and vitamin C treatment improves fibrosis in patients with nonalcoholic steatohepatitis. Am J Gastroenterol 2003;98:2485–2490.

[12] Barnard PJ, Baker MV, Berners-Price SJ, Day DA. Mitochondrial permeability transition induced by dinuclear gold(I)-carbene complexes: potential new antimitochondrial antitumour agents. J Inorg Biochem 2004;98:1642–1647.

[13] Zhao L, Zhang C, Zhuo L, Zhang Y, Ying JY. Imidazolium salts: a mild reducing and antioxidative reagent. J Am Chem Soc 2008;130:12586–12587.

[14] Harlow KJ, Hill AF, Welton T. Convenient and general synthesis of symmetric N,N'-disubstituted imidazolium halides. Synthesis 1996;6:697–698.

[15] Vogel S, Piantedosi R, Frank J, Lalazar A, Rockey DC, Friedman SL, Blaner WS. An immortalized rat liver stellate cell line (HSC-T6): a new cell model for the study of retinoid metabolism *in vitro*. J Lipid Res 2000;41:882–893.

[16] Zhang C, Zhuo L. Epigallocatechin gallate and genistein attenuate glial fibrillary acidic protein elevation induced by fibrogenic cytokines in hepatic stellate cells. Int J Mol Med 2006;18:1141–1151.

[17] Halliwell B, Whiteman M. Measuring reactive species and oxidative damage in vivo and in cell culture: how should you do it and what do the results mean? Br J Pharmacol 2004;142:231–255.

[18] Padillo FJ, Cruz A, Navarrete C, Bujalance I, Briceno J, Gallardo JI, Marchal T, Caballero R, Tunez I, Muntane J, Montilla P, Pera-Madrazo C. Melatonin prevents oxidative stress and hepatocyte cell death induced by experimental cholestasis. Free Radic Res 2004;38:697–704.

[19] Whalen R, Rockey DC, Friedman SL, Boyer TD. Activation of rat hepatic stellate cells leads to loss of glutathione S-transferases and their enzymatic activity against products of oxidative stress. Hepatology 1999;30:927–933.

[20] Baur JA, Pearson KJ, Price NL, Jamieson HA, Lerin C, Kalra A, Prabhu VV, Allard JS, Lopez-Lluch G, Lewis K, Pistell PJ, Poosala S, Becker KG, Boss O, Gwinn D, Wang M, Ramaswamy S, Fishbein KW, Spencer RG, Lakatta EG, Le Couteur D, Shaw RJ, Navas P, Puigserver P, Ingram DK, de Cabo R, Sinclair DA. Resveratrol improves health and survival of mice on a high-calorie diet. Nature 2006;444: 337–342.

[21] Frei B, Higdon JV. Antioxidant activity of tea polyphenols *in vivo*: evidence from animal studies. J Nutr 2003;133: 3275S–3284S.

[22] Droge W. Free radicals in the physiological control of cell function. Physiol Rev 2002;82:47–95.

[23] Hou Z, Sang S, You H, Lee MJ, Hong J, Chin KV, Yang CS. Mechanism of action of (−)-epigallocatechin-3-gallate: auto-oxidation-dependent inactivation of epidermal growth factor receptor and direct effects on growth inhibition in human esophageal cancer KYSE 150 cells. Cancer Res 2005;65:8049–8056.

[24] Lin LC, Hung LC, Tsai TH. Determination of (−)-epigallocatechin gallate in rat blood by microdialysis coupled with liquid chromatography. J Chromatogr A 2004;1032: 125–128.

[25] Keum YS, Chang PP, Kwon KH, Yuan X, Li W, Hu L, Kong AN. 3-Morpholinopropyl isothiocyanate is a novel synthetic isothiocyanate that strongly induces the antioxidant response element-dependent Nrf2-mediated detoxifying/antio xidant enzymes in vitro and in vivo. Carcinogenesis 2008;29: 594–599.

[26] Peng J, Stevenson FF, Doctrow SR, Andersen JK. Superoxide dismutase/catalase mimetics are neuroprotective against selective paraquat-mediated dopaminergic neuron death in the substantial nigra: implications for Parkinson disease. J Biol Chem 2005;280:29194–29198.

[27] Floyd RA. Nitrones as therapeutics in age-related diseases. Aging Cell 2006;5:51–57.

[28] Nakae D, Uematsu F, Kishida H, Kusuoka O, Katsuda S, Yoshida M, Takahashi M, Maekawa A, Denda A, Konishi Y, Kotake Y, Floyd RA. Inhibition of the development of hepatocellular carcinomas by phenyl N-tert-butyl nitrone in rats fed with a choline-deficient, L-amino acid-defined diet. Cancer Lett 2004;206:1–13.

This paper was first published online on iFirst on 7 August 2009.